Presented at the 29th European PV Solar Energy Conference and Exhibition, 22-26 September 2014, Amsterdam, The Netherlands

TWO IMAGE PROCESSING TOOLS TO ANALYSE ALKALINE TEXTURE AND CONTACT FINGER GEOMETRY IN MICROSCOPE IMAGES

Theresa Strauch, Matthias Demant, Andreas Lorenz, Jonas Haunschild, Stefan Rein
Fraunhofer-Institute for Solar Energy Systems (ISE),
Heidenhofstr 2, 79110 Freiburg, Germany

ABSTRACT: For texture quality assessment, a detailed microscopic analysis acts as a valuable addition to reflection measurements. The pyramidal surface structure of alkaline texture is suitable to be characterized by geometric parameters. After metallization, microscopic measurements also contribute to the assessment of printing results. The latter depend on the surface of the solar cell and are thus interconnected with texture surface properties. In the following, two tools are presented which allow a combined quantification of texture and contact finger geometry. Relevant parameters are identified for this purpose and the conformity of these parameters with manual evaluations and established measurement methods is demonstrated. Pyramids are detected with high precision for diverse textures (97±2%) and the contact finger parameters agree with reference methods (relative deviation of ±2%). The combined analysis is found suitable to investigate the relation between texture and contact finger parameters.
Keywords: Characterisation, Image Processing, Metallization, Shading, Texturization

1 INTRODUCTION

Microscopic measurements play an important part for a deeper understanding of texturization and metallization results respectively relations between both aspects, as recently suggested in [1],[2]. Confocal microscopes allow 3D-records of the samples: The surface profile (height profile image) of the sample is scanned layer by layer, while optical information is recorded as well (confocal images).

Until now, results on the basis of those measurements are mainly attained by manual evaluation, which is time-consuming, prone to errors and hardly reproducible. Investigations with regard to quantifiable relations can only be achieved by automatic evaluations with large sets of samples. Therefore, algorithms are required that yield relevant parameters for the characterization of texture and contact finger geometry and thus data for a reliable and statistically representative quantitative evaluation. These algorithms have to be robust with respect to differences in illumination, presence or absence of untextured regions, transmission of microscope lens etc. [3]. If these challenges are met, this may allow a deeper insight in the relation between texture surface morphology and contact finger formation during the printing process.

In previous publications, texture parameters were extracted and analysed with regard to their distribution [9] and their relation to solar cell performance [4]. It was found that the more homogeneous the texture, the better the cell parameters. For this purpose, parameters characterising homogeneity were defined and extracted automatically. Besides, it was found that untextured areas also contribute to quality losses.

Contact finger features going along with high quality are given by good electrical conduction and low shading losses. In geometric terms, this means that the finger should be narrow, but aspect ratio (height-to-width-ratio) and cross section area should be high, in order to reduce electrical losses related to line resistance [5]. Furthermore, industrial throughput and material costs are important economic aspects. Different printing technologies have been developed to approach an optimum in metallization, e.g. screen printing (which is well established in industry), stencil printing [6] and dispensing [7]. To assess the quality of these methods, information about cross-section area, shading and core-effective width of the contact fingers is essential. Small cross-section areas increase line resistance and if the periphery of the contact finger is flat, it hardly contributes to electrical conduction. Geometrical evaluation via image processing algorithms helps to explain the behaviour of the electrical conduction in the contact finger, thereby enriching the inline measurements of electrical parameters.

In the following, we will present the algorithm outlines and define the relevant parameters, then we will demonstrate results of different sample types, discuss the significance and consistency of the parameters and finally present results regarding the relation between the analyzed texture and contact finger geometry.

2 APPROACH

After defining the parameters for texture and contact finger respectively, the outline of the algorithms will be introduced. Comparative measurements and the approach to investigate the relation between texture and stencil-printed contact fingers are presented afterwards.

2.1 Texture parameters

Alkaline texture is characterised by pyramids (the faces of these pyramids being the most stable crystal surface configuration) whose edges, which we will call segments, are visible in the confocal image. The whole pyramid thus stands out as a bright cross whose centre, i.e. the intersection of the segments, is the pyramid peak (cf. Fig. 1). The parameters and their descriptions are listed in Table 1, a visualization is given in Fig. 1.

Table 1: Definition of texture geometry parameters

Parameter	Description
$l_{min}\,[\mu m]$	Minimal segment length
$l_{max}\,[\mu m]$	Maximal segment length
$l_{mean}\,[\mu m]$	Mean segment length
$A\,[\mu m^2]$	Base area of a pyramid
$d_{loc}\,[\mu m]$	Local peak distance
$R_a\,[\mu m]$	Arithmetic mean roughness, cf. Eq. (1)
$R_z\,[\mu m]$	Roughness depth, cf. Eq. (2)

The segment lengths l_{min}, l_{max} and l_{mean} indicate the height difference between peak and basis of each segment. Besides this height information, the statistic eval-

uation provides important information about homogeneity. We will discern between intra-pyramidal and inter-pyramidal homogeneity. The first considers the shortest, longest and mean segment length for every single pyramid; a distance measure of intrapyramidal inhomogeneity is given by l_{max}-l_{min}. The more regular the pyramid(s), the smaller this difference [4]. Interpyramidal homogeneity is characterised by global statistic values (standard deviation, scattering) of l_{mean}. The mean distance d_{loc} (respectively its standard deviation) is another suitable parameter to measure homogeneity. It is calculated by means of the local density. For ideal and homogeneously distributed pyramids it corresponds to the mean segment length.

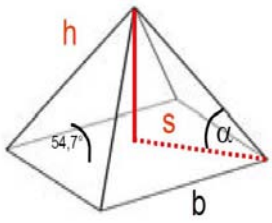

Figure 1 a) Model of a texture pyramid, taken from [4]; the segment s is the pyramid edge projected onto the base area; as α=45°, the height h has the same length as s

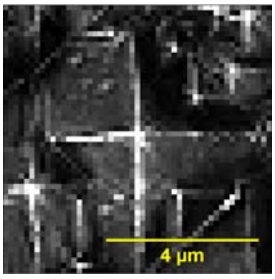

Figure 1 b) Excerpt of confocal microscope image with typical pyramid cross; smaller pyramids are grouped around the larger one (50x-lens, 3.67px/µm)

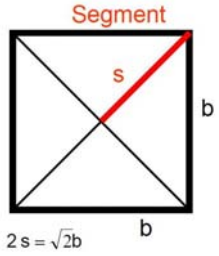

Figure 1 c) Sketch of the projection onto the base area [4] of the pyramid with the same segment as in 1 a); the base area with equidistant segments is a square in the ideal case

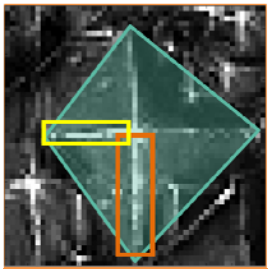

Figure 1 d) Examples of relevant parameters for the larger pyramid: shortest (yellow) and longest (orange) segments, convex hull (green)

The pyramid base area A is either defined as the convex hull of the segments, as shown in Fig. 1 d), or as non-overlapping joining regions, the confinements of these regions consisting of the meeting pyramid faces. We call the first "Area Definition 1" and the second "Area Definition 2" in the following. The base area and its standard deviation constitute a good measure for homogeneity with either definition.

Roughness parameters were calculated according to the following equations (line integration, as given here, can be replaced by area integration):

$$R_a = \int_{x_1}^{x_2} |h(x) - \bar{h}| dx \qquad (1)$$

$$R_z = \frac{1}{n-2} \sum_{i=2}^{n-1} h_{max,i} - h_{min,i}, \qquad (2)$$

where $h(x)$ is the height at position x, $\bar{h}$ is the mean over the whole line and $h_{max,i}$ and $h_{min,i}$ are the maximum resp. minimum over the i^{th} part of the measuring line. These values were calculated on the basis of the microscopic height profile images, integrating both over lines and areas.

2.2 Finger geometry parameters

An ideal finger is geometrically characterised by a high aspect-ratio [5], which means that the finger height should be high compared to the finger width. In this ideal case, the shading-relevant finger width is identical with the conduction-effective core finger width, i.e., the covered cell area should be small compared to the finger volume. In reality, the lateral margins of the finger are characterised by bleed-out areas which are caused by a leakage of the paste into the texture. The cross-section area is mainly responsible for the line resistance of the contact finger and thereby gives a physical background for the algorithm. Contact finger height and shading-relevant finger width are therefore important parameters as well as core finger width and conduction-effective cross-section-area. For the calculation of the underground surface one has to rely on approximations, since the microscopic image only provides information about the contact finger surface.

Fig. 2 and Table 2 give an overview over the relevant contact finger parameters. The finger cross-section area is determined using the height profile image and allows connecting finger height with area as a projected volume. Therefore, the cross-section area A_{crsct} is the basis for calculating the conduction-effective core finger width w_{cond}, which constitutes the width of the projected finger volume mainly responsible for the conductivity. The local finger height h is the vertical maximum of the local cross-section profile (smoothed because the finger surface is rough). In most cases w_{sh} is significantly larger than w_{cond} due to paste bleeding effects. The aspect ratio is calculated from the shading width and the finger height.

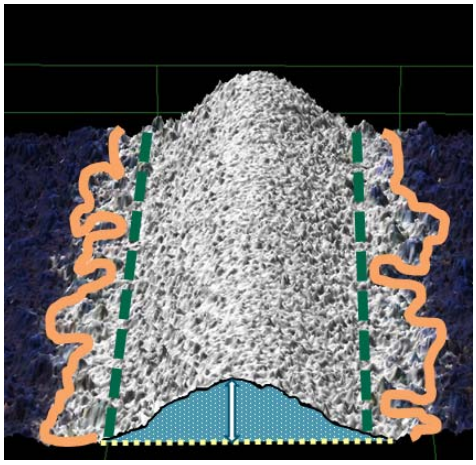

Figure 2: Contact finger excerpt with relevant parameters: bleed-out-regions (orange) confining the shading area of the finger, core conducting zone (confined by dark green dashed lines), local cross-section area A_{crsct} (structured blue) and local height h (white arrow) based on the local linear interpolation of the underlying surface (dotted bright line; 3D aspect of confocal microscope image).

Table 2: Definition of contact finger geometry parameters

Parameter	Description
$A_{crsct}\,[\mu m^2]$	Local cross-section area
$w_{sh}\,[\mu m]$	Local shading width
$w_{core}\,[\mu m]$	Local conduction-effective finger width
$h_{min}\,[\mu m]$	Minimal height over whole finger
$h_{max}\,[\mu m]$	Maximal height over whole finger
$h\,[\mu m]$	Local height over whole finger
$\bar{h}\,[\mu m]$	Mean height over whole finger

2.3 Algorithms

The tools "TEXANA" and "FINEUP" were implemented in MATLAB. The texture analysis tool TEXANA is partly based on the one in [4]. Both analysis tools provide graphic user interfaces, offering options to change settings for different measurement conditions, to visualize results of individual images and compute results for a whole image stack.

The algorithm for texture analysis then consists of two steps: peak detection and pyramid reconstruction. If existent in the image, the contact finger area must be excluded from texture analysis beforehand. Bright spots in the image of calculations are equally excluded since their origin is undefined. Peak detection is realized via a preprocessing step: anisotropic diffusion, smoothing the back-ground while conserving the bright pyramid segments, and a filter which detects lines and in this way the pyramid segments. For more detail we refer to [4]. The detected peaks undergo an additional check, which differs according to Area Definitions 1 and 2. According the area definitions, we discern two ways of reconstruction whose visualization results can be seen in the excerpt of an example image (Fig. 3):

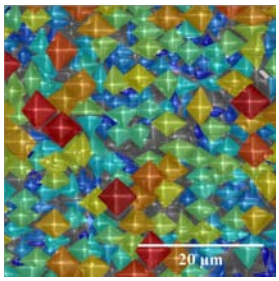

a) Visualization of pyramid areas according to Area Definition 1

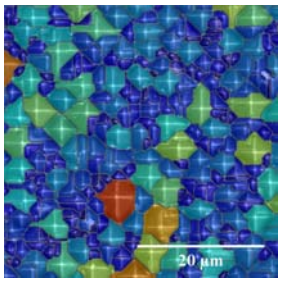

b) Visualization of pyramid areas according to Area Definition 2

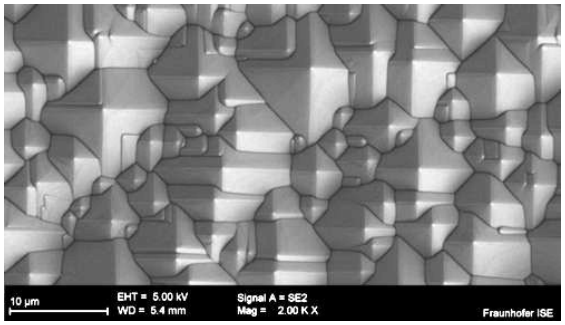

c) SEM image of similar texture

Figure 3: Visualization of pyramid areas according to the two definitions and reconstruction mechanisms.

1. Pyramid segment reconstruction via edge hysteresis, as realized in [4]; this reconstruction reassembles parts of the same segment, broken apart by image noise; using the confocal image.
2. Reconstruction of complete profile with ideal pyramids starting at detected pyramid peaks whose height is given in the height profile image.

The outline of the algorithm for the contact finger geometry is the following: Firstly, the reflecting part of the image is detected in the confocal image, i.e. the shading area. Secondly, the roughness and waviness of the texture in direct neighborhood to this area are extrapolated such that the underground of the contact finger may be estimated on either lateral side. The extrapolation is necessary because obviously the finger profile interferes with the estimation of the underground. The extrapolated values on either side can now be interpolated linearly to give a rough estimation of the wafer surface beneath the contact finger. The height profile is adjusted accordingly (cf. Fig. 4).

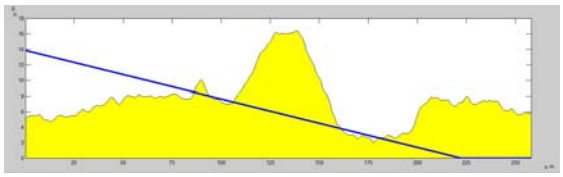

Figure 4: Example height profile through finger (yellow) with interpolating linear function (blue); The area above the dark line is recognized as contact finger shape by the algorithm, excluding the profile parts disconnected with the regions of maximal heights.

2.4 Experimental setup

The evaluation is based on confocal microscope images of metallized solar cells. These images were recorded using the Olympus LEXT 6. We organised the samples in several experimental groups. A definition of a selection among these groups is given in Table 3. The vertical range recorded by the 3D-scan of the microscope has an impact on accuracy of the height profile image; contact fingers increase this range in relation to texture. To take this effect into account, images containing only texture information were compared along with images containing contact finger information. The printing technique used for the greatest part of our samples was stencil-printing [4]. For comparison with printing results of other technologies, dispensed fingers [8] were analysed using the same algorithm.

In order to establish the validity of the defined parameters, several measurements were used for comparison: The most important, though certainly not always most reliable way is the comparison by eye. This especially concerns texture homogeneity, the comparative contemplation of texture roughness with different samples, but also the hit ratio of the pyramids achieved by the algorithm. Judgment by eye also helps to get a good setting for stack analysis.

By using incorporated features of the microscope software for manual analysis, parameters like height difference and cross-section area can be extracted along profile lines. This is a good validation method for comparison with automatically calculated data.

Table 3: Definition of the sample groups; the abbreviation "metalliz. rec." means that the image contains part of a contact finger along with texture. The number of samples ranged from 20 to 37 images per group.

Properties	**Group definitions**			
	1	2	3	4
Metalliz. rec.: Stencil Pr.	x	x		
No metalliz. rec.			x	x
Homog. textured	x			x
Mixed texture		x	x	
Small pyr. dominate			x	x
Medium pyr. dominate	x			
Large pyr. dominate		x		

For texture, roughness measurements are an established method to get information about the surface. The caveat of this measurement is obvious: It is not directly related to the geometry properties, because regions with pyramids are recorded along with eventual pyramid-free regions. With an intact texture, however, roughness values should correlate with the segment length data. Two of the common parameters describing the roughness are listed in Table 1 and in Equations (1) and (2).

Microscopic measurements realized with a Scanning Electron Microscope (SEM) can serve for comparison as well: This measurement enables an accurate description of the surface, so that e.g. pyramid height can be measured with high precision for selected spots.

For inline measurements of electrical cell parameters and their respective relations to texture and finger geometry we refer to [3] and [4].

2.5 Relation between texture and finger geometry

Stencil printing results on different textures were examined with respect to finger and texture geometry. A more detailed description of the methods can be found in [3], the focus of that publication being the relation between texture roughness and contact finger geometry respectively electrical parameters.

3 RESULTS

3.1 Texture parameter results

The accuracy of finding the pyramid peaks strongly influences the reliability of the extracted parameters. It can be indicated by means of *recall* and *precision*: The first is the ratio *found true positives/actual number of positives*, the second is given by *found true positives/all found positives*. Precision and recall of the pyramid finding process depend on the measurement parameters, but also on the texture itself. For almost all samples of the defined groups precision and recall ranged between 95% and 100% with a mean of 97% and a median of 98%. Although precision and recall were generally higher when no contact finger was part of the image as well, the only case for which the algorithm did not yield reliable results was the case of very fine texture and contact finger in the same image. However, the analysis of a large amount of different samples (not belonging to the defined groups) made it obvious that non-intact textures with partly destroyed pyramids, terraced pyramid edges and areas of tiny pyramids reduce both recall and precision, the concrete values depending on the degree of these effects; for example, slightly terraced pyramids still allow a recall of about 90% and a precision of 90-95%, but stronger damage reduces both values to unacceptably low values, making the algorithm inapplicable. Further, it was found that over-illuminated images decrease precision, whereas a weak illumination decreases recall.

It was noticed that many small pyramids are rejected with the reconstruction method according to Area Definition 1 and thus not involved in the evaluation. We also found that these rejected pyramids were often close to the resolution limit, which restricts a stable calculation with well-discernable values. As it is often ambiguous whether the candidates are indeed pyramid peaks or not, we did not consider pyramids of a size close to the resolution limit (approx. 0.25µm for a 50x lens in our case) when counting the pyramids, but only those which are unambiguously pyramids.

Average results for l_{min}, l_{max}, l_{mean}, A and d_{loc} are shown in Table 4. They were in good agreement with SEM data and evaluation by eye.

Table 4: Average texture parameters for the defined groups, according to the area definitions

Average of parameter	**Area Def.**	**Groups**			
		1	2	3	4
l_{min} (µm)	1	1.46	2.02	1.15	1.02
	2	1.45	1.45	1.04	0.83
l_{max} (µm)	1	4.64	5.85	2.73	2.71
	2	3.46	4.20	2.35	2.14
l_{mean} (µm)	1	2.84	3.74	1.92	1.83
	2	2.40	2.83	1.66	1.44
A (µm²)	1	14.48	24.83	6.71	6.07
	2	14.30	21.16	6.92	5.64
d_{loc} (µm)	1	5.96	7.07	3.79	3.71
	2	5.34	6.72	3.80	3.49
R_z (µm)	2	4.10	9.51	1.66	1.85

3.2 Consistency regarding the area definitions

Texture parameters were checked for consistency and the results according the two different area definitions were compared.

Segment length and area are obviously related. With Area Definition 1, the upper limit of the area is $A(P_i) < 2\, l_{mean}(P_i)$, where $l_{mean}(P_i)$ is the mean segment length for the pyramid P_i, with equality in the case that both pyramid diagonals have the same length. Thus, the closer the ratio of area and the function of the mean segment length is to 1, the more regular are the pyramids. With Groups 1-4, the average ratio $A(P_i)/(2\, l_{mean}(P_i))$ is about 0.88 with Area Definition 1, which confirms consistency, and about 1.25 with Definition 2.

In spite of those different results for this ratio, the average and median of the base area itself were very similar with both area definitions, indicating that the average mean segment length is larger with Method 1.

Furthermore, roughness must be consistent with segment length, unless a significant part of the surface are is determined by untextured parts. R_a showed a significant correlation with the standard deviation of the mean segment length, (with a correlation R^2=0.985 for Method 1,

Method 2 slightly lower), and R_z was shown to correlate with the maximum segment length (R^2=0.98 for Method 1, Method 2 significantly lower). The roughness values were calculated with the algorithm, but they were calibrated according to results of a measuring device called "Perthometer" which scans the surface roughness along a profile line.

For the most part, the histograms of the extracted parameters show a left-skewed distribution (cf. Fig. 5). Interpyramidal homogeneity differences were most evident in the standard deviation of base area. The difference between Groups 1 and 2 with regard to the latter were very large, ranging between 25% (relative to maximum value) and 50%. But also the standard deviation differences of d_{loc} showed similarly high values. These two parameters seem to be suitable to characterise homogeneity. Intrapyramidal homogeneity was large (between 80% and 130% of the mean segment length) throughout all groups, the individual pyramids thus deviating significantly from ideal pyramids.

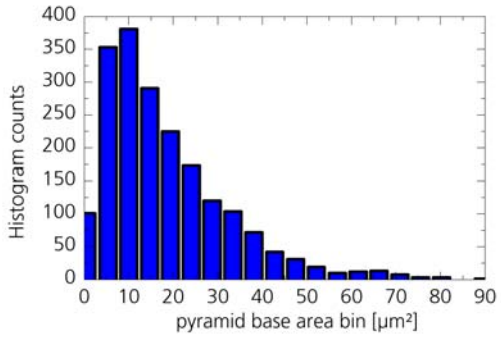

Figure 5: Histogram of pyramid area (20 bins) for a sample from Group 3

3.3 Finger parameter results

The geometric parameters of the contact finger differed in the way that was expected, according to the printing techniques – w_{sh} being smaller and closer to w_{cond} with dispensed fingers than with stencil printed fingers.

The comparison with manual contact finger evaluations was realized using tools incorporated in the microscope software (for example LEXT OLS4000), for Groups 1 and 2 as well as for samples with other kinds of texture (not among the groups defined here: plasma texture, acid texture). The relative deviations from the manually evaluated data generally ranged between 1-3% (with regard to the maximum value) for width estimation (both w_{sh} and w_{cond}), as well as for maximum and average height h_{max} and h_{mean}. For h_{min} the deviations were considerably larger with 7-20%. This large deviation of h_{min} can be explained with the estimation of the textured underground beneath the finger: By eye, the minimal height position is estimated according to the original height information, but the original height often differs significantly from the height after the adjustment according the estimated underground.

3.4 Relation between finger and texture geometry

Opposite to our expectations, the ratio between the length of the actual finger outline and the length of the ideal outline did neither correlate with any of the texture data, nor did the difference between core and shading area width confirm some relation of this kind. However, a correlation of shading width and different texture parameters seems very likely, the correlation-R^2-values ranging from 50-60% (cf. Fig. 6).

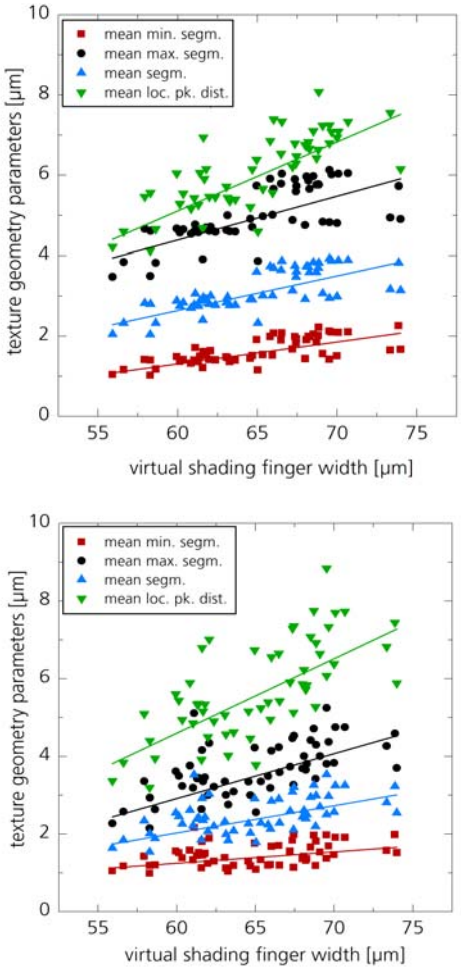

Figure 6: Results with respect to the reconstruction methods according to Area Definitions 1 (above) and 2 (below). Texture parameters plotted against virtual shading area of the finger: average minimum, maximum segment length, average segment length and mean local peak distance (abbr.: mean loc. pk. dist.); linear approximations plotted as lines, calculated via a regular least-squares fit.

4 DISCUSSION

Precision and recall differ especially with fine texture. Partly we could attribute this to the height resolution which is restricted by the maximal vertical difference scanned by the microscope. As all images for the combined analysis of texture and contact finger geometry were recorded with a 50x lens, very fine texture also reaches resolution confinements within the surface area.

Moreover, with the refinement of the peak candidates according to Area Definition 1, small pyramids are often rejected. This can possibly distort the notion of homogeneity, but it helps to establish more robust values for the unambiguous peaks. Many very small pyramids are but artefacts of larger pyramids and it is questionable whether they can indeed be seen as individual pyramids.

With Area Definition 2, the peaks of smaller pyramids are accepted for the most part. Thus, in terms of

cardinal number the small pyramids get an overweight, which decreases the mean, but also the median value of the segment length parameters. This even outweighs the effect that the base area may contain regions outside the convex hull and could thus attain larger values – which also explains the "unphysical" values of the ratio $A(P_i)/(2\, l_{mean}(P_i))$ with Area Definition 2.

Both reconstruction methods have their field of application: The first is recommendable if one is interested in robust data that characterises texture, especially when comparing one dataset to another or when investigating possible relations with other parameters. The second is appropriate if one is rather interested in the distribution of pyramids, in their number and homogeneity. Moreover, it can deal with effects of fluctuations of the profile on larger scale, like the so-called "elephant feet": pyramids can be unusually elongated in the direction of the well.

The distribution of texture parameters was partly inhomogeneous, but for the most part left-skewed with a peak near zero, strongly monotonically increasing, weakly monotonically decreasing. In a previous publication [9], distributions of similar, but not identical texture parameters were evaluated with the statistic program "EasyFit". The pyramid height relative to neighbour pyramids was characterized by a Fatigue-Life-Distribution, but for similar distributions as those resulting for our parameters, no appropriate distribution was found. As the skew to the left is probably caused by restricted resolution, it may be assumed that the distributions should approach a Gaussian curve on the logarithmic scale.

5 CONCLUSION AND OUTLOOK

We developed two tools for texture and contact finger geometry analysis that can process stacks of confocal microscope images and produce robust results. Those parameters have been shown to be appropriate to characterize texture and contact finger geometry: They were consistent among themselves and in good agreement with other evaluation methods. Contact finger parameters show reasonable and traceable differences between different printing methods.

The correlation between texture and finger geometry is shown to be likely. Printing processes undergo a lot of variation, so, to get representative sets of data, many more samples will be necessary to significantly prove our assumptions. The software tools are adequate to carry out such complex investigations.

ACKNOWLEDGEMENTS

This work has been supported by the German ministry of economics under the frame of the "QUASSIM-PLUS" project (FKZ: 0325493A), for which we thank all project partners. Further, the authors would like to thank Katharina Schneider and Gunter-Tobias Barnes-Hofmeister for their dedicated measurements and for the tests with the software.

REFERENCES

[1] M. Aoki et al., in 39th IEEE Photovoltaic Specialists Conference Tampa. 2013.

[2] A. Ryan and H. Lewis, Effect of Surface Roughness on Paper Substrate Circuit Board, IEEE Trans. Compon., Packag. Manufact. Technol. **2(**7), S. 1202–1208, 2012.

[3] A. Lorenz, Influence of Texture Roughness on Solar Cell Front Side Metallization using Stencil Printing Technology, to be submitted.

[4] K. Birmann, M. Demant, and S. Rein, in 26th EUPVSEC Hamburg..

[5] M. Pospischil et al., Paste Rheology Correlating With Dispensed Finger Geometry, IEEE Journal of Photovoltaics **4(**1), S. 498–503, 2014.

[6] B. Heurtault and J. Hoornstra, in 25th EUPVSEC Valencia.

[7] X. Chen, K. Church, and H. Yang, in 35th IEEE Photovoltaic Specialists Conference Honolulu.

[8] M. Pospischil et al., in 39th IEEE Photovoltaic Specialists Conference Tampa. 2013.

[9] E. Wefringhaus, C. Kesnar, and M. Löhmann, Statistical Approach to the Description of Random Pyramid Surfaces using 3D Surface Profiles, Proceedings of the SiliconPV 2011 Conference (1st International Conference on Crystalline Silicon Photovoltaics) **8(**0), S. 135–140, 2011.